processes

MDPI

Article

Real-Time Estimation of CO_2 Absorption Capacity Using Ionic Conductivity of Protonated Di-Methyl-Ethanolamine (DMEA) and Electrical Conductivity in Low-Concentration DMEA Aqueous Solutions

Sang-Jun Han, Joo Young Han and Jung-Ho Wee *

Department of Energy and Environmental Engineering, The Catholic University of Korea, 43 Jibong-ro, Wonmi-gu, Bucheon-si 14662, Gyeonggi-do, Republic of Korea; hsj8812@chungbuk.ac.kr (S.-J.H.); dbstjd5679@naver.com (J.Y.H.)

* Correspondence: jhwee@catholic.ac.kr or jhwee@korea.ac.kr; Tel.: +82-2-2164-4866

Abstract: The present study investigates the real-time estimation of CO_2 absorption capacity (CAC) based on the electrical conductivity (EC) of low-concentration di-methyl-ethanolamine (DMEA) solutions (0.1–0.5 M). CO_2 absorption experiments are conducted to measure the variation in CAC and EC during CO_2 absorption, revealing a strong correlation between the two properties. The ionic conductivity of $DMEAH^+$ formed during absorption is calculated to be 53.1 $S{\cdot}cm^2/(mol{\cdot}z)$, which is found to be larger than that of $TEAH^+$ and $MDEAH^+$. This can be attributed to the smaller molar mass and higher ionic mobility of $DMEAH^+$. A significant finding is that the measured EC (EC_M) of the DMEA solutions consistently demonstrates a lower value than the theoretically predicted value. This discrepancy is due to the larger ionic size of $DMEAH^+$, which results in a reduction in the real mean ionic activity coefficient. This effect becomes more pronounced with increasing DMEA concentration. Consequently, a higher CAC is required to produce the same change in EC at higher amine concentrations. Based on these findings, an empirical equation is devised to estimate CAC from EC_M in solutions of constant DMEA concentration. This equation will be employed as a practical approach for the in situ monitoring of CO_2 absorption using DMEA aqueous solution.

Keywords: carbon capture and storage; di-methyl-ethanolamine; CO_2 absorption; ionic conductivity; electrical conductivity; correlation

check for updates

Citation: Han, S.-J.; Han, J.Y.; Wee, J.-H. Real-Time Estimation of CO_2 Absorption Capacity Using Ionic Conductivity of Protonated Di-Methyl-Ethanolamine (DMEA) and Electrical Conductivity in Low-Concentration DMEA Aqueous Solutions. *Processes* **2024**, *12*, 2495. https://doi.org/10.3390/pr12112495

Academic Editors: Georgios Bampos, Vijaya Raghavan and Georgios Karanikolos

Received: 5 September 2024
Revised: 5 November 2024
Accepted: 8 November 2024
Published: 10 November 2024

Copyright: © 2024 by the authors. Licensee MDPI, Basel, Switzerland. This article is an open access article distributed under the terms and conditions of the Creative Commons Attribution (CC BY) license (https://creativecommons.org/licenses/by/4.0/).

1. Introduction

Carbon dioxide (CO_2)—which is emitted from a variety of industrial processes, including fossil fuel combustion, cement production, and steel and chemical plants—constitutes a significant contributor to global warming. CO_2 constitutes approximately 76% of global greenhouse gas emissions, with annual emissions reaching 37.15 billion metric tons [1,2]. In July 2023, the UN Secretary-General underscored the urgency of the current climate change crisis, asserting that the era of global warming has concluded and that we have entered the period of "global boiling" [3]. To address climate change, ongoing research over the past 30 years has focused on the development of carbon dioxide capture and storage (CCS) technologies, which are characterized by high economic viability and performance. Various CCS methods, including bioconversion [4–7] and adsorption using novel materials [8–12], have been investigated; however, these approaches frequently fail to achieve the desired impact at a large scale. Among the various CCS technologies, chemical absorption using alkanolamine has been extensively studied over an extended period, and it is currently the only technology that has been successfully commercialized with the objective of addressing the urgent climate crisis [13–17].

Alkanolamines are a class of substances that contain both amino (-NH_2, -NHR, and -NR_2) and hydroxyl (-OH) functional groups. They are highly and selectively reactive with

CO_2, and they can be classified as primary, secondary, and tertiary amines based on the number of R groups they contain. An absorption process using mono-ethanolamine (MEA), a member of the primary amine group, has been commercialized due to its rapid reaction rate and low cost [18–22]. However, the reaction of MEA with CO_2 limits the theoretical maximum amine utilization to 0.5 mol CO_2/mol amine in high amine-concentrated solutions. Moreover, MEA is highly corrosive to equipment, requiring a significant amount of energy to strip the CO_2 from the absorbent (or to regenerate the solutions). An alternative approach is being investigated in which tertiary amines are utilized as absorbents. Although these amines, such as tri-ethanolamine (TEA), methyl-di-ethanolamine (MDEA), and di-methyl-ethanolamine (DMEA), have been reported to have relatively low reaction rates, they achieve a maximum amine utilization of 1.0 mol CO_2/mol amine, are relatively less corrosive, and require minimal energy for CO_2 stripping. Most studies using tertiary amines as the absorbent have concentrated on their blending effect with primary or secondary amines to enhance the performance of the absorbents [23–27]. However, there has been a relative lack of research into the specific absorption performance and properties of tertiary amine solutions, which would be expected to furnish crucial insights for the continued advancement of absorbents.

Recent advances in sensor technology have demonstrated the potential of low-cost, real-time monitoring systems to enhance data collection for environmental and industrial processes. For example, low-cost sensors have been employed to monitor spatial and temporal pollution in urban areas, providing a practical solution for large-scale exposure assessments [28]. One study highlighted that the use of a dispersion model enabled the testing of dust pollution distribution in a seaside town, thereby significantly enhancing pollution monitoring [29]. In water quality monitoring, electrochemical sensors have emerged as a crucial tool due to their capacity to transduce chemical interactions into electrical signals, thereby enabling real-time, multi-parameter monitoring, which is feasible even in resource-limited settings [30,31]. Similarly, electrolytic conductivity sensors, which are widely used in diverse industries, offer reliable and precise monitoring of electrolytes in various applications [32,33]. Given these advantages, we opted to employ electrical conductivity (EC) measurements as an effective and economical method for the real-time estimation of CO_2 absorption capacity in aqueous DMEA solutions. In this way, we utilize the advantages of EC sensors to provide a practical solution for the continuous monitoring of CO_2 absorption processes in industrial settings.

In this context, the present study investigated the CO_2 absorption performance and electrical characteristics of the CO_2 absorption system using DMEA aqueous solution with a relatively low concentration of DMEA (0.1–0.5 M). First, the ionic conductivity (IC) value of protonated DMEA ($DMEAH^+$) generated from the chemical absorption reaction between CO_2 and DMEA—which was achieved through a series of absorption experiments—was presented. The relationship between the CO_2 absorption capacity (CAC) (or the amount of CO_2 absorbed) and the EC of the solution at the arbitrary absorption time was also established for each solution, which finally resulted in the derivation of a general empirical equation for predicting the amount of CO_2 absorbed based on EC measurements of the solutions.

2. CO_2 Absorption Mechanism Using DMEA Aqueous Solutions

In the DMEA solutions prepared for the CO_2 absorption, a small amount of the DMEA molecule first receives H^+ from the water to become $DMEAH^+$ and OH^- in the solution, as expressed in Equation (1) [34,35].

$$DMEA + H_2O \leftrightarrow DMEAH^+ + OH^- \quad (1)$$

The two ionic concentrations are determined from DMEA's base dissociation constant (pK_b) of 4.78 [36]. If CO_2 is then added to the DMEA solution to be absorbed, two reactions occur, as summarized in Equations (2) and (3) [34,35,37].

$$OH^- + CO_2 \rightarrow HCO_3^- \quad (2)$$

$$DMEA + H_2O + CO_2 \rightarrow DMEAH^+ + HCO_3^- \quad (3)$$

When CO_2 is injected into the DMEA solution, OH^-, which is generated via Equation (1), reacts with CO_2 according to Equation (2), thereby resulting in the formation of HCO_3^-. Subsequently, CO_2 is absorbed by reacting with OH^- in the H_2O activated by DMEA molecules to produce $DMEAH^+$ and HCO_3^-, as expressed in Equation (3). The CO_2 absorption mechanism in tertiary amine aqueous solution is designated as the "base-catalyzed reaction" for CO_2 hydration [38]. This is illustrated in Figure 1.

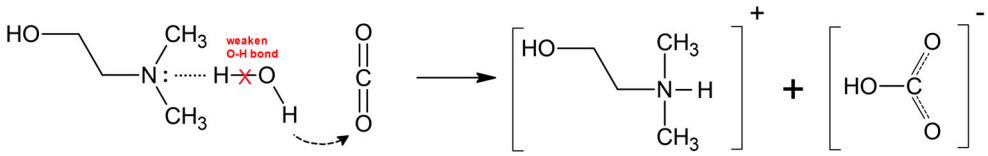


Figure 1. Reaction mechanism for CO_2 absorption in di-methyl-ethanolamine (DMEA) aqueous solutions.

In the absorption process, the DMEA molecule does not directly react with CO_2; instead, a lone pair of electrons on the nitrogen atom of DMEA forms hydrogen bonds with water molecules (illustrated by the dotted line in Figure 1), which activates the hydroxide ion (OH^-) on the opposite side of the water molecule. This enhances its reactivity with the injected CO_2 molecule. Consequently, the formation of $DMEAH^+$ and HCO_3^-, as well as their zwitterion ($DMEAH^+ \cdot HCO_3^-$), occurs in the solution during CO_2 absorption. Additionally, CO_2 can be physically absorbed into the water component, as described in Equation (4), which is referred to as the amount of physical absorption of CO_2; this is also included in the total CAC of the solutions [39,40].

$$H_2O(l) + CO_2(g) \rightarrow H_2CO_3(aq) \quad (4)$$

The amount of CO_2 physical absorption under experimental conditions (25 °C, 1 atm, and a CO_2 partial pressure of 0.33 atm) is 0.023 mol CO_2/L of pure distilled water [41]. The H_2CO_3 produced by physical absorption increases the concentration of either HCO_3^- or CO_3^{2-} according to the pH of the solution. However, both concentrations are very small compared to those of the ions produced by the chemical absorption reaction (Equations (2) and (3)), so they are not included in the calculation of the EC of the solutions.

3. Experimental Methodology and Calculations

3.1. Experimental Setup for CO_2 Absorption

Figure 2 shows a schematic diagram of the absorption experiment with DMEA solution.

The experimental setup, including the equipment and methods used in this study, was established identically to that used in our previous work on other amine-based solutions [41–43]. The details of the setup are described below.

A cylindrical semi-batch reactor (D: 110 mm; h: 80 mm; total volume: 0.76 L) maintained at 25 °C by a jacket connected to a water circulator was filled with 0.5 L of 0.1–0.5 M DMEA (99.5%, Sigma-Aldrich, St. Louis, MO, USA) aqueous solution. Next, the empty space in the reactor was filled with N_2 gas (99.9%) and completely sealed to confirm tightness. For CO_2 absorption, N_2 and CO_2 gasses (99.99%) were passed through a gas mixture (D: 90 mm; h: 400 mm; total volume: 2.55 L) at respective flow rates of 2.0 and 1.0 L/min using a mass flow controller (MFC; TSC-200, MKPrecision, Siheung-si, Republic of Korea). This resulted in a gas mixture with a CO_2 concentration of 33.3 vol%. Prior to absorption,

this gas mixture was bypassed from the reactor through a three-way valve installed at the top of the reactor, after which its CO_2 concentration was checked using a CO_2 analyzer (maMos-200, Madur Electronics, madur Polska Sp. z o. o., Zgierz, Poland). The gas mixture was then used as the absorption gas.

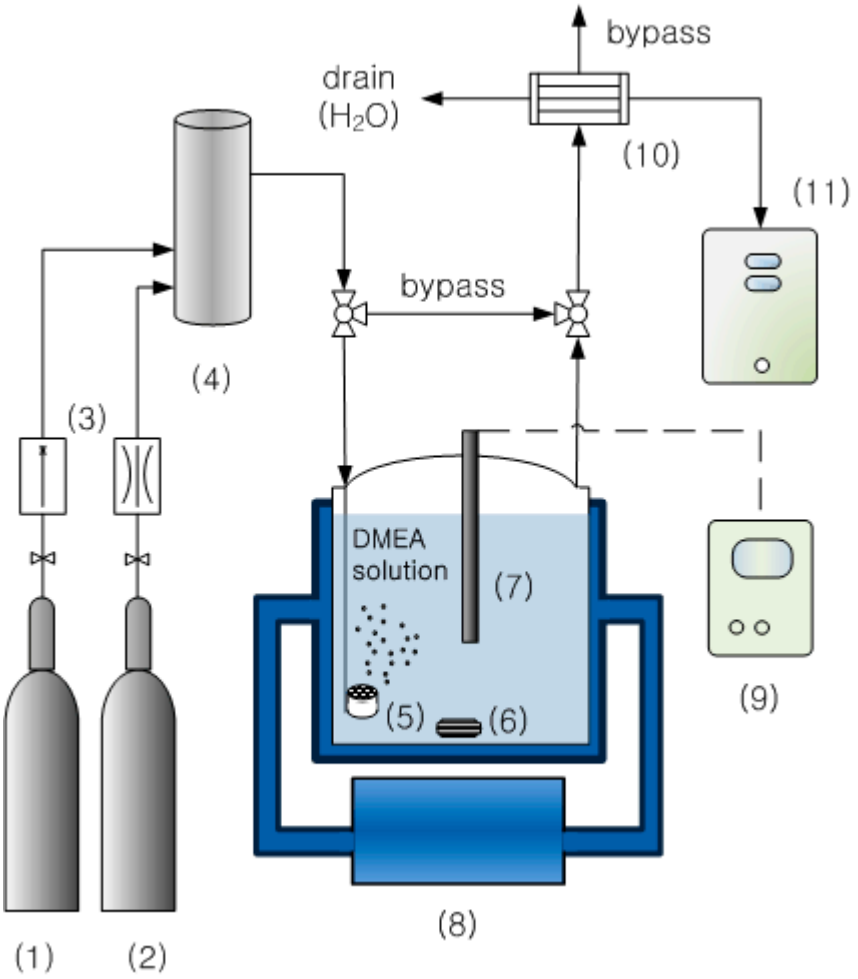


Figure 2. The experimental apparatus for CO_2 absorption using DMEA aqueous solutions. (1) N_2 cylinder, (2) CO_2 cylinder, (3) mass flow controller (MFC), (4) gas mixture, (5) bubbler, (6) magnetic stirrer, (7) pH/EC sensor, (8) water circulator, (9) pH/EC meter, (10) humidifier, (11) CO_2 gas analyzer.

When the gas mixture was injected into the reactor, a glass fiber bubbler with a pore size of 1 um was fixed at the end of the inlet gas line. This was carried out to ensure uniform contact between the solution and the gas. The solution was stirred at 380 rpm using a magnetic stirrer while absorbing. A pH/EC meter (Orion 4 Star, Thermo Scientific, Waltham, MA, USA) was also used to measure the variations in the pH and the EC of the solution caused by CO_2 absorption in real time at 5 s intervals. The CO_2 concentration in the outlet gas from the reactor was measured using a CO_2 analyzer. The absorption completion point was determined as the point at which the CO_2 concentration in the outlet gas was equal to the initial CO_2 concentration of the inlet gas.

3.2. Calculation of Electrical Conductivity (EC) of the CO_2-Absorbed DMEA Solutions

The EC of a CO_2-absorbed solution was calculated using Equations (5)–(10) below [44–48].

$$\mathrm{EC(S/m)} = k_o \gamma^2, \tag{5}$$

$$k_o = \sum z_i \lambda_i c_i, \tag{6}$$

$$IS = 500\sum c_i {z_i}^2, \tag{7}$$

$$\log\ \gamma = -Az_+z_-\sqrt{IS} \qquad (\text{IS} < 0.01), \tag{8}$$

$$\log\ \gamma = -Az_+z_-\frac{\sqrt{IS}}{1+\sqrt{IS}} \qquad (0.01 \le \text{IS} \le 0.1), \tag{9}$$

$$\log\ \gamma = -Az_+z_-\left(\frac{\sqrt{IS}}{1+\sqrt{IS}} - 0.2IS\right) \qquad (0.1 < \text{IS} \le 0.5), \tag{10}$$

The EC of a CO_2-absorbed solution is the product of the EC of an infinitely diluted solution (k_o: (S/m)) and the square of the mean ionic activity coefficient (γ), as described in Equation (5) [44,45]. First, the value of k_o is calculated via Equation (6), using the absolute charge (z), ionic conductivity (λ: S·m^2/mol·z), and concentration (c: mol/m^3) of ion i in solution. Secondly, the value of γ can be calculated selecting one of Equations (8)–(10) depending on the ionic strength (IS: mol/L) value of the solution, which can be calculated from Equation (7) [46–48]. Here, A is a Debye–Huckel constant—0.509 (kg/mol)$^{0.5}$ at 25 °C. Therefore, three factors are required to calculate the EC of a CO_2-absorbed solution—the concentration, charge value, and IC of the ions in the solution.

3.3. Calculation of Ionic Conductivity of DMEAH$^+$

As CO_2 is absorbed into the DMEA solution, the ions produced or consumed are OH^-, $HCO_3{}^-$, and $DMEAH^+$, and the charge value of these ions is 1. Of these, the ICs of OH^- and $HCO_3{}^-$ have previously been reported in the literature as 198.6 and 44.50 S·cm^2/(mol·z), respectively [49,50]. However, the IC value of $DMEAH^+$ is not yet known; therefore, it is essential to know in order to calculate the EC value of the solution in accordance with the absorption reaction. The variation in the concentration of ions present in the solution is also necessary to calculate the EC value of the solution during the absorption reaction. Since the concentration of ions in the solution can be estimated based on the amount of CO_2 chemical absorption measured in real time using Equations (2) and (3), the EC variation in the solution during the absorption can be calculated after determining the IC of $DMEAH^+$. To find the IC of $DMEAH^+$, the initial guess value was assumed to be 1, and it was increased by increments of 0.01 until reaching the IC of H^+, which is the largest value (349.8 S·cm^2/(mol·z)) among all the ions [51]. Then, the EC was repeatedly calculated via Equation (5) (referred to as EC_C). Finally, the EC_C value was determined as the value entered at the time when the mean absolute percentage error (MAPE) between the EC_C value and the measured EC (EC_M) was minimized. The MAPE between the EC_M and the EC_C value during the absorption in 0.1–0.5 M DMEA solution was calculated using Equation (11) [52].

$$\text{MAPE}(\%) = \frac{100}{n}\sum_{i=1}^{n}\frac{|\text{EC}_\text{M} - \text{EC}_\text{C}|}{\text{EC}_\text{M}}, \tag{11}$$

The calculation was performed using MATLAB 2024a.

4. Results and Discussion

4.1. CO_2 Absorption Performance of 0.1–0.5 M DMEA Aqueous Solutions

The CAC and EC_M of the 0.1–0.5 M DMEA solutions according to time are shown in Figure 3a and Figure 3b, respectively.

The CAC of the solution varied with the shape of the square root function; the slope here refers to the CO_2 absorption rate. The initial absorption rates of all solutions were steep. However, as time progressed, the slope gradually decreased until absorption was completed. This is because the amine concentration in the solution is high at the beginning of absorption, but as the absorption progresses, the concentration decreases as the amine is consumed, as expressed in Equation (4). The trend of EC_M variation according to time, shown in Figure 3b, is also similar to that of CAC, which indicates that the EC_M value

of the solution is directly affected by the concentration of ions generated by the CO_2 absorption reaction.

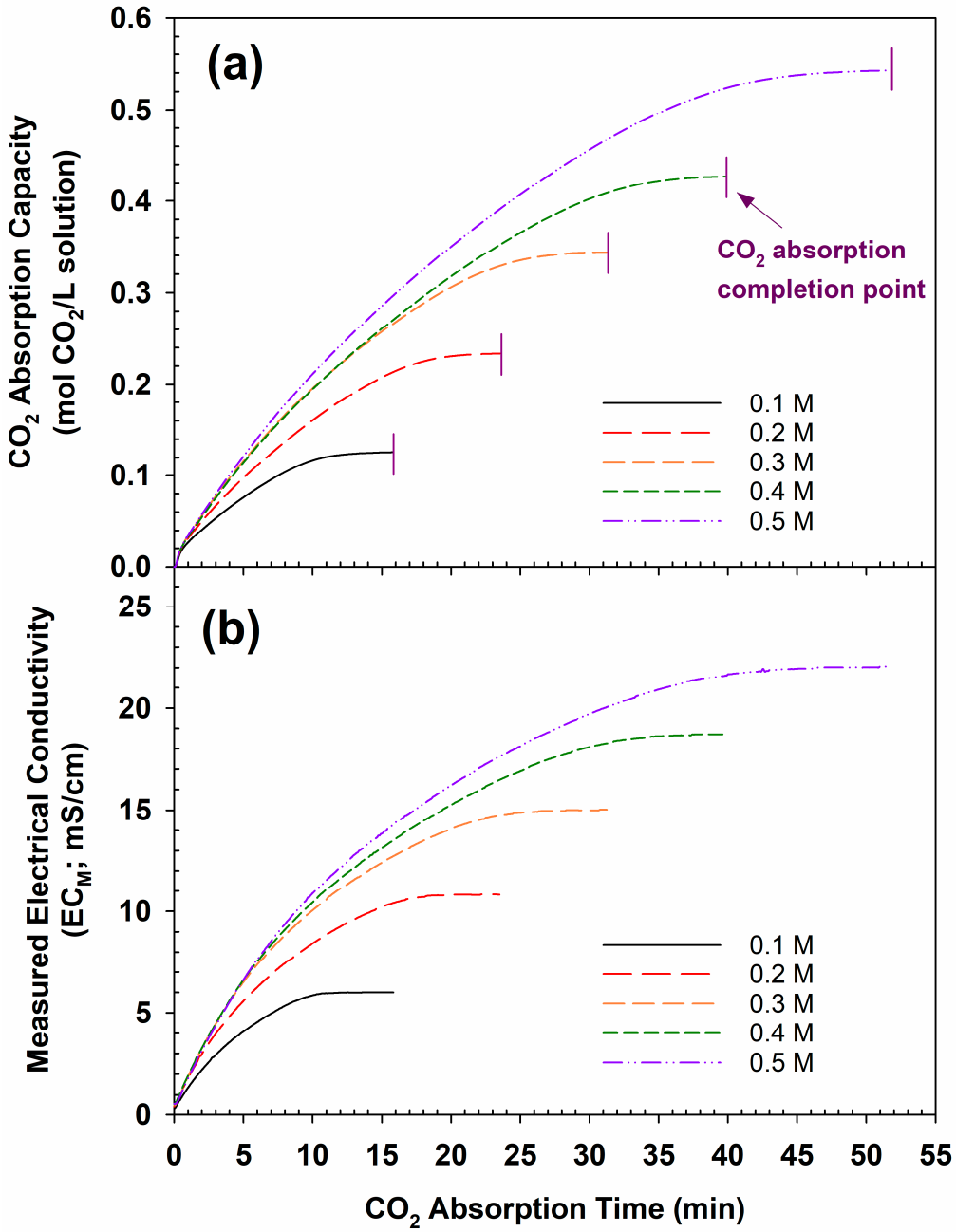


Figure 3. (**a**) CO_2 absorption capacity (CAC) and (**b**) measured electrical conductivity (EC_M) as a function of CO_2 absorption time in 0.1–0.5 M DMEA solutions.

Table 1 summarizes the total CAC of 0.1–0.5 M DMEA solutions at the absorption completion point, the amount of chemical and physical absorption, the total absorption time, and the average slope of Figure 3a, i.e., the overall CO_2 absorption rate of the solutions.

Here, the total CAC is the sum of the CO_2 chemical absorption, which is stoichiometrically calculated based on the DMEA concentration using Equations (2) and (3), and the CO_2 physical absorption given in Equation (4), which is calculated by subtracting the amount of chemical absorption from the total CAC. The amount of CO_2 physical absorption was at its lowest at 0.032 mol CO_2/L in a 0.1 M solution, whereas it was at its highest at 0.050 mol CO_2/L at 0.5 M. This amount is slightly higher than that of pure distilled water (0.023 mol/L), as referenced in Section 2, and it increases proportionally to the amine

concentration. This is because the HCO_3^- produced by the chemical absorption of CO_2 with DMEA in the solution shifts the equilibrium point of the carbonate ions in the solution, which can produce more H_2CO_3 or CO_3^{2-} in the solution than in pure distilled water; consequently, additional trace amounts of CO_2 are absorbed.

Table 1. Total, chemical, and physical CO_2 absorption capacities (CACs), total absorption time, and overall CO_2 absorption rate in 0.1–0.5 M DMEA solutions.

	Initial Amine Concentration of DMEA Solution (mol/L)				
	0.1	**0.2**	**0.3**	**0.4**	**0.5**
Total CAC (mol CO_2/L)	0.135	0.238	0.345	0.448	0.550
Chemical CAC (mol CO_2/L)	0.100	0.200	0.300	0.400	0.500
Physical CAC (mol CO_2/L)	0.035	0.038	0.045	0.048	0.050
CO_2 absorption time (min)	15.0	23.8	35.0	44.9	52.8
Overall CO_2 absorption rate (mmol CO_2/(L·min))	9.0	10.0	9.9	10.0	10.4

The average standard deviation of CAC and CO_2 absorption time is ±0.012 and ±0.5, respectively.

Although the overall CO_2 absorption rate was slightly lower at 9.0 mmol CO_2/(L·min) in the 0.1 M solution, the overall absorption rate converged to about 10.0 mmol CO_2/(L·min), regardless of the initial amine concentration in the solution. This is consistent with previous studies on the kinetics of tertiary amines, which have shown similar behavior [53–56]. For example, W. Jiang et al. reported a pseudo-first-order rate constant of 1.5–3.0 s^{-1} in 0.075–0.175 M DMEA solutions, corresponding to a second-order rate constant of 22.19 m^3/(kmol·s) [53]. This indicates that the reaction is more dependent on CO_2 concentration than on DMEA concentration. This is attributed to the fact that DMEA, as a tertiary amine, follows a base-catalyzed reaction mechanism that facilitates the reaction of H_2O with CO_2. Therefore, the absorption rate is more dominated by the CO_2 concentration than the DMEA concentration in the solution. Thus, at relatively low concentrations of 0.5 M or less, the absorption rate was not found to be insensitive to the concentration of DMEA.

4.2. Ionic Conductivity of Protonated DMEA ($DMEAH^+$)

The IC and charge values of the ions produced from the CO_2 absorption reaction (Equations (2) and (3)), including the dissociation reaction (Equation (1)) of the DMEA solution, are presented in Table 2.

Table 2. Ionic conductivity, absolute value of electric charge, and molar mass of ions generated from chemical CO_2 absorption in DMEA solutions with other tertiary amine solutions.

Ions	**Ionic Conductivity (S·cm²/(mol·z))**	**Absolute Value of Electric Charge (z)**	**Molar Mass (g/mol)**	**Reference**
OH^-	198.6	1	17.0	[49]
HCO_3^-	44.5	1	61.0	[50]
$DMEAH^+$	53.1	1	90.1	This work
$MDEAH^+$	46.5	1	120.1	[41]
$TEAH^+$	37.6	1	150.1	[41]

As mentioned in Section 3.3, the IC of the OH^- and HCO_3^- ions have previously been shown to be 198.6 and 44.5 S·cm²/(mol·z), respectively [49,50]. However, the IC of $DMEAH^+$ was not identified in the published literature. Consequently, in this study, the IC of $DMEAH^+$ was calculated using the trial-and-error method described in Section 3.3. This calculation was based on the ionic concentrations calculated from the amount of CO_2 chemical absorption (as determined using Equations (2) and (3)), as well as the EC_M. The calculated IC of $DMEAH^+$, as determined in this study, is 53.1 S·cm²/(mol·z) with an MAPE of 13.06%. The IC of $DMEAH^+$, as determined by the present study, is larger than the values that have been reported for the other two of the three kinds of tertiary

amines, namely $TEAH^+$ (37.6 $S{\cdot}cm^2/mol{\cdot}z$) and $MDEAH^+$ (46.5 $S{\cdot}cm^2/mol{\cdot}z$), in prior studies [41]. These values are inversely proportional to the molar masses of the three ions, which is likely attributable to the observation that the smaller and lighter ion with the same charge generally exhibits increased mobility in solution. This is consistent with the results of previous research, which has indicated that an increase in ionic mobility leads to an increase in ionic conductivity [57]. Moreover, as the range of absolute values obtained for IC in the case of $DMEAH^+$ is similar to that of the other two tertiary protonated amines, the result of the IC of $DMEAH^+$ obtained herein may be considered to be reliable.

4.3. EC_C and EC_M Variation According to CO_2 Absorption in 0.1–0.5 M DMEA Solutions

When using the IC of $DMEAH^+$ (53.1 $S{\cdot}cm^2/mol{\cdot}z$), the theoretical EC values of 0.1–0.5 M DMEA solutions, as calculated using Equation (5), are shown in Figure 4, along with the variation in EC_M (Figure 3b).

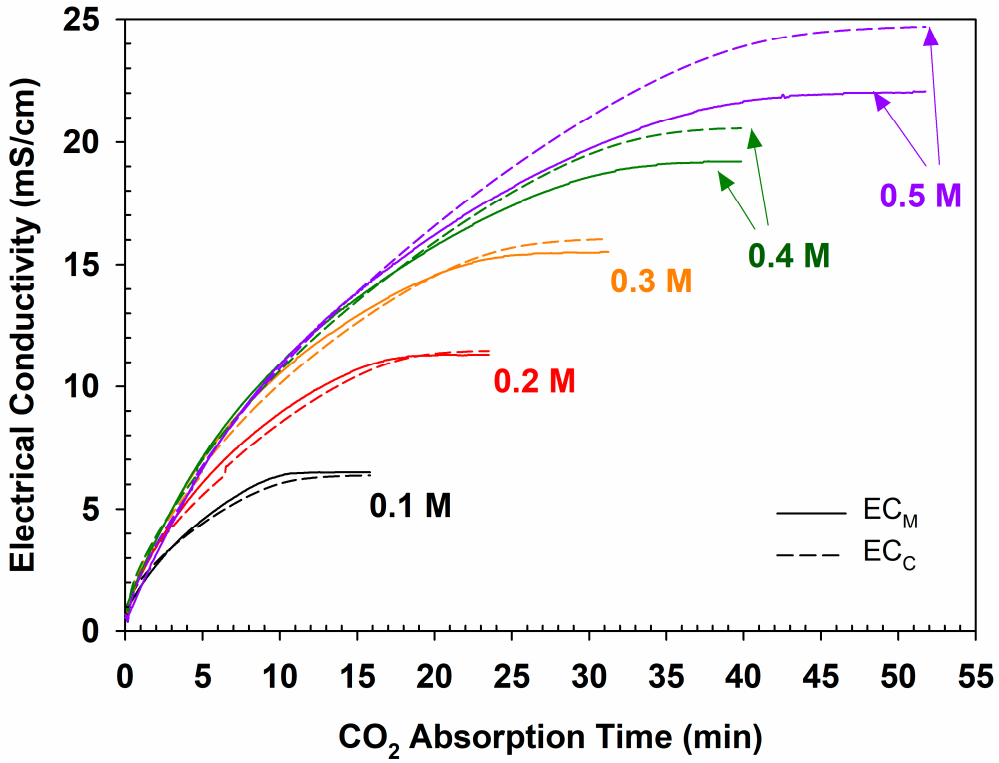


Figure 4. Comparison of measured electrical conductivity (EC_M) and calculated electrical conductivity (EC_C) during CO_2 absorption in 0.1–0.5 M DMEA solutions.

As can be seen in Figure 4, the variations in EC_M and EC_C were similar for all solutions. However, as CO_2 absorption neared completion, the discrepancy between the two EC values increased with the initial amine concentration. For example, at the absorption completion point of 0.1 M solution, the EC_M and EC_C values were 6.00 and 5.88 mS/cm, respectively, with an MAPE of 2.1%. In contrast, for a 0.5 M solution, the EC_M and EC_C values were 22.07 and 24.70 mS/cm, respectively, with an associated MAPE of 11.9%. These results are attributed to the tertiary amine nature of the $DMEAH^+$, the molecular structure of which is large and complex, resulting in a reduced mean ionic activity coefficient in the solution compared to that predicted using Equation (10). Sami-ullah et al. investigated the relationship between molecular weight and the activity coefficient in ionic liquid systems, revealing an inverse proportionality between the two [58]. H.-N Jeon et al. developed an artificial neural network-based model to predict the infinite dilution activity coefficients of organic molecules, utilizing parameters such as molecular structure, polarizability, and hydrogen bonding [59]. The results of our research also exhibited a similar trend to those of previous studies. Thus, as the concentration of amines increased, the mean ionic activity

coefficient decreased, and this was accompanied by an increase in the difference between the EC_M and EC_C values, with the EC_M being measured at a lower value than the EC_C. However, in contrast to the other solutions, the EC_M was slightly higher than the EC_C in the 0.1 M solution, and it also had the smallest MAPE. This is due to the relatively very low concentration, as well as the fact that EC_M is augmented by the EC derived from the trace amount of CO_3^{2-} or HCO_3^- generated through the physical absorption process.

4.4. Correlation Between CO_2 Absorption Capacity and Electrical Conductivity

The trend in variations in CAC and EC_M according to absorption time was highly similar for the 0.1–0.5 M DMEA solutions, as illustrated in Figure 3a,b. The correlation between the CAC and the EC_M of the solution measured at the same time is depicted in Figure 5a, while the results of their regression analysis are presented in Figure 5b.

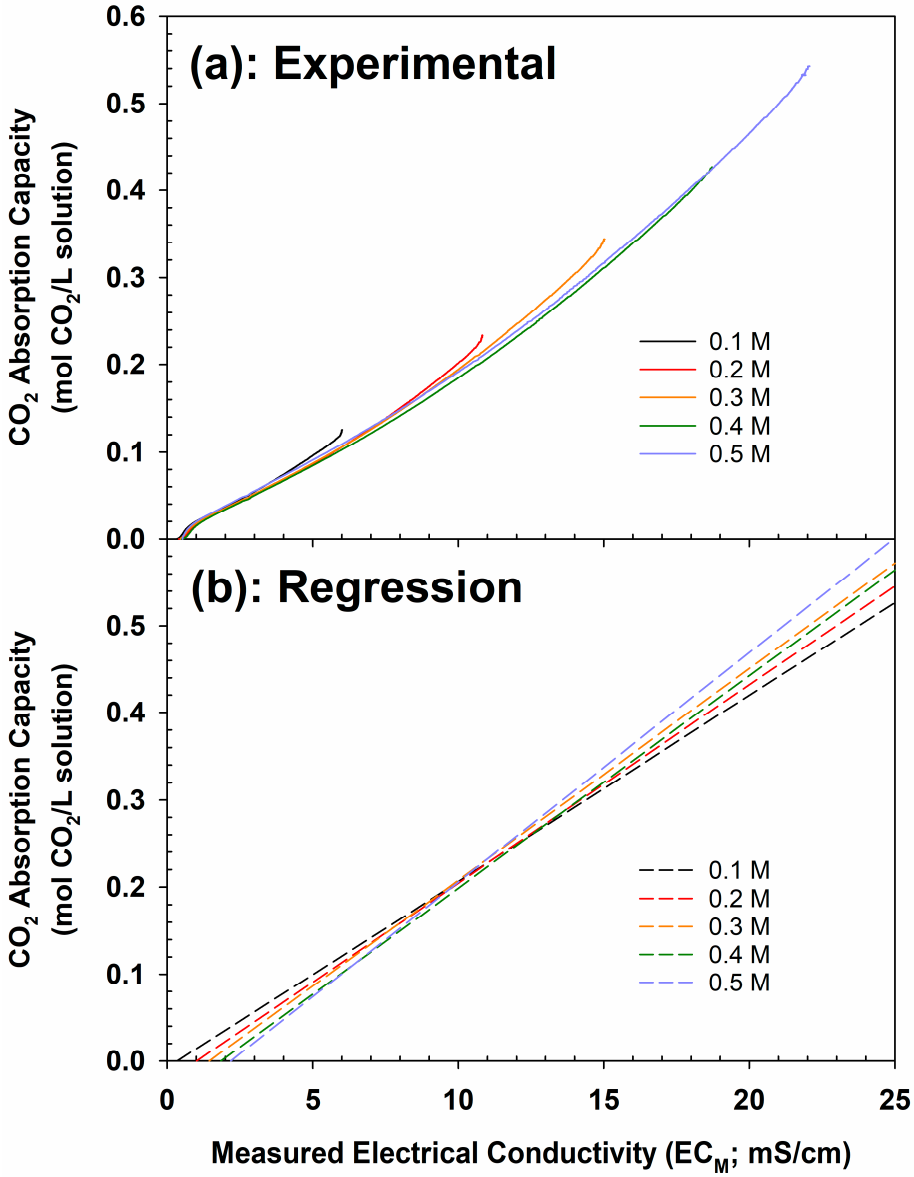


Figure 5. (**a**) Relationship between CO_2 absorption capacity (CAC) and measured electrical conductivity (EC_M) during CO_2 absorption and (**b**) linear regression analysis for 0.1–0.5 M DMEA solutions.

The correlation between CAC and EC_M in all solutions was linear, which indicates that EC_M was linearly proportional to CAC, and that both were directly related to the ionic (or molecular) concentration in the solution. This is valid for all CO_2-absorbed

DMEA solutions with concentrations of 0.1–0.5 M, which showed linearity in the CAC and EC_M of the solution. As a result, the correlation equation between the two variables was derived through regression analysis (Figure 5b), and can be expressed as shown in Equation (12) below.

$$CO_2 \text{absorption capacity}(\text{CAC; mol}CO_2/\text{L}) = a \cdot EC_M + b, \quad (12)$$

The slope (a) and y-intercept (b) of Equation (12) were calculated for all solutions and summarized according to the initial amine concentration (C_{DMEA}) of the solution; these values are presented in Figure 6a,b.

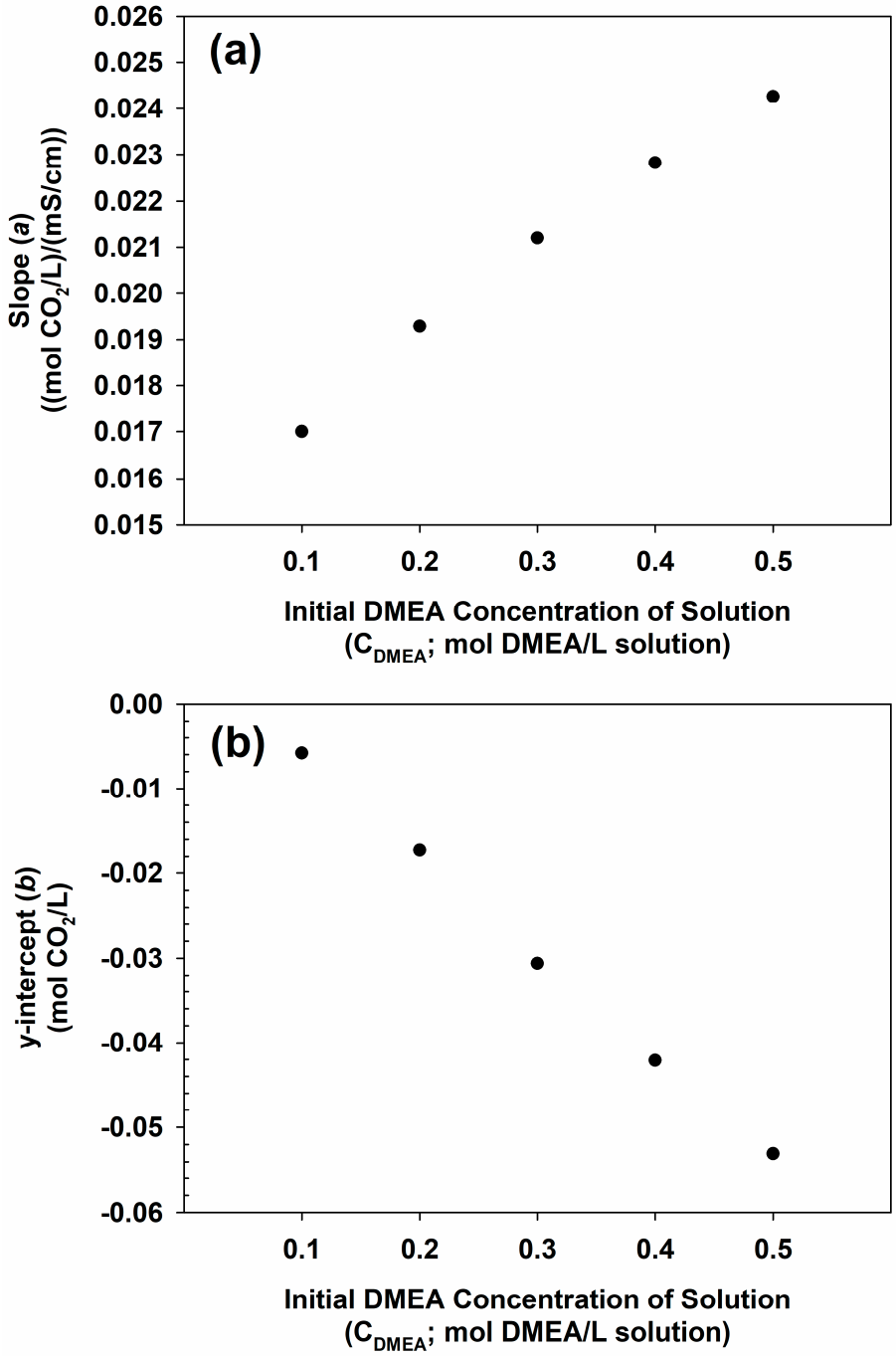


Figure 6. (**a**) Slope and (**b**) y-intercept values from the linear regression analysis between measured electrical conductivity (EC_M) and CO_2 absorption capacity (CAC) in 0.1−0.5 M DMEA solutions.

The slope (a) and y-intercept (b) exhibited linear proportionality to the initial amine concentration in solution. Here, the slope represents the requisite CO_2 absorption capacity (mol CO_2/L) in solution to achieve a 1 mS/cm increase in the EC of the solution, which exhibits a proportionality to the initial amine concentration of solutions (Figure 6a), as evidenced by the relation expressed in Equation (13).

$$\text{slope}(a; (\text{mol}CO_2/\text{L})/(\text{mS}/\text{cm})) = 0.0181 \cdot C_{DMEA} + 0.0155, \quad (13)$$

The y-intercept (b) value of Equation (12) shown in Figure 6b decreased proportionally to the initial amine concentration, and the correlation coefficient was found to be 0.998 as a result of a linear regression, thus indicating a highly linear relationship with respect to the initial amine concentration. The correlation between the two variables was expressed as shown in Equation (14).

$$\text{y} - \text{intercept}(b; \text{mol}CO_2/\text{L}) = -0.1193 \cdot C_{DMEA} + 6.0 \cdot 10^{-3}, \quad (14)$$

The y-intercept value represents the amount of CO_2 absorbed when the EC of the solution is zero. However, even before CO_2 absorption, a constant EC value for the DMEA solutions could be observed due to the presence of $DMEAH^+$ and OH^- ions in the solution, with a certain concentration, as described in Equation (1). Consequently, the y-intercept value is merely a mathematical representation of the correlation between EC and CAC.

Therefore, the slope and y-intercept of Equation (12) could, respectively, be generalized from Equations (13) and (14) for 0.1–0.5 M DMEA solutions to derive an empirical equation that estimates the CAC of each solution as a function of the EC_M and initial amine concentration, as shown in Equation (15).

$$\begin{gathered} CO_2 \text{ absorption capacity}(\text{mol } CO_2/\text{L}) = 0.0181 \cdot C_{DMEA} \cdot EC_M + 0.0155 \cdot \\ EC_M - 0.1193 \cdot C_{DMEA} + 6.0 \cdot 10^{-3}, \end{gathered} \quad (15)$$

Shown above, Equation (15) may be used for the estimation of CAC in real time based on the variations in the EC of DMEA solutions of the given initial amine concentration. Finally, Figure 7 illustrates the relative behavior of the CAC (y-axis) of DMEA solutions in terms of the C_{DMEA} ranging from 0.1 to 0.5 M (z-axis), as well as the EC_M value of the solution (x-axis). Moreover, this Figure presents variations in the amount of saturated CO_2 absorbed and the maximum EC_M value of each solution (parameters), and the data presented in Figure 7 provide information in relation to the relative behavior and interactions of the three variables in this system.

The correlation equation among CAC, EC_M, and DMEA concentration demonstrates that EC_M can serve as a reliable indicator for estimating CAC in real systems in real time, providing practical insights for CCS technologies. Recent studies emphasize the significance of such empirical models in enhancing the efficiency of CO_2 capture systems through real-time monitoring and control capabilities [13,60,61]. This approach has been confirmed to be applicable to other amine systems, including MEA, AMP, and TEA [41,42]. Consequently, this research offers a methodology for optimizing CCS processes by utilizing the variation in EC_M of DMEA solutions, establishing a reliable empirical model, and investigating their electrical properties.

However, the results are limited in two main respects. First, the research focused on low-concentration (0.1–0.5 M) DMEA solutions, which are considerably lower than those typically employed in industrial contexts. Second, the research was conducted under a restricted range of conditions, considering a single pressure and temperature to determine the ionic conductivity of $DMEAH^+$, which limits the scope for providing more detailed data on CO_2 absorption. Therefore, future research focuses on extending the experimental conditions to cover a broader range of amine concentrations, temperatures, and pressures. Furthermore, it is essential to incorporate a numerical model based on vapor–liquid equilibrium (VLE) simulations for the amine–CO_2–H_2O system to enhance the

predictive capabilities of the electrical conductivity in the electrolyte model. Additionally, future research should focus on the application of more comprehensive models, such as the extended Non-Random Two-Liquid (NRTL) or Universal Quasi-Chemical (UNIQUAC) models that consider both long- and short-range interactions, and the traditional Debye–Huckel model that mainly considers long-range interactions.

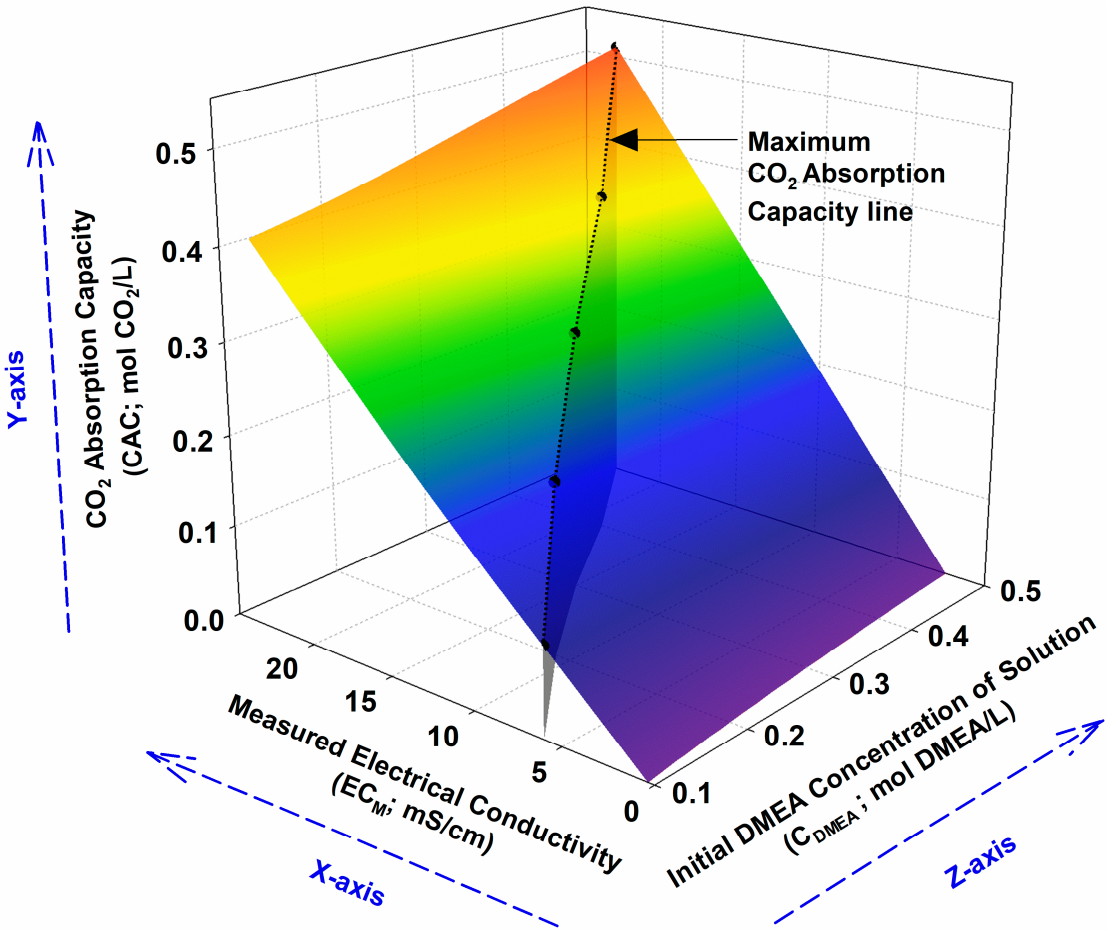


Figure 7. Variation in CO_2 absorption capacity (CAC; y-axis) as a function of initial DMEA concentration (C_{DMEA}; z-axis, ranging from 0.1 to 0.5 M) and measured electrical conductivity (EC_M; x-axis) in CO_2-absorbed DMEA solutions.

5. Conclusions

The present study investigated the CO_2 absorption characteristics of low-concentration (0.1–0.5 M) DMEA solutions, aiming to develop an empirical equation for the real-time estimation of CO_2 absorption capacity (CAC) based on the electrical conductivity (EC) of these solutions. A laboratory-scale semi-batch reactor was employed to evaluate the CO_2 absorption performance and the variation in EC of DMEA solutions during CO_2 absorption.

As CO_2 was absorbed into the DMEA solution, the measured electrical conductivity (EC_M) of the solution and CAC varied similarly over time, providing a basis for predicting CAC through changes in the EC_M. The overall CO_2 absorption rate for 0.1–0.5 M DMEA solutions was approximately 10.0 mmol CO_2/(L·min), independent of DMEA concentration. This consistency arises because the amine concentration is very low, while the absorption reaction follows a base-catalyzed mechanism predominantly influenced by CO_2 concentration. Moreover, the ionic conductivity (IC) of protonated DMEA ($DMEAH^+$) was determined to be 53.1 $S{\cdot}cm^2/(mol{\cdot}z)$, which was larger than that of other tertiary amines such as $TEAH^+$ (37.6) and $MDEAH^+$ (46.5). This outcome can be attributed to $DMEAH^+$ having the smallest molar mass among them. In the case of the 0.1 M DMEA solution

saturated with CO_2, the EC_M was greater than the theoretically calculated EC (EC_C). This discrepancy is due to the low amine concentration and the presence of trace amount of HCO_3^- and CO_3^{2-} ions formed from physically absorbed CO_2. However, for 0.2–0.5 M DMEA solutions, the EC_M is lower than the EC_C. This discrepancy increased with higher DMEA concentrations. This can be explained by the larger ionic size of $DMEAH^+$, resulting in the actual mean ionic activity coefficient being smaller than the theoretical value as the concentration increases. Furthermore, the CAC required to increase the EC_M of the DMEA solution by 1 mS/cm increases proportionally with the initial amine concentration. This is due to the decreased activity of ions at higher concentrations, necessitating the production of a larger amount (concentration) of ions through absorption for a given change in EC.

Finally, the empirical equation derived from this study offers a practical approach for estimating CAC from EC measurements in DMEA solutions, enhancing the efficiency of CO_2 absorption processes through the real-time monitoring of CAC. However, limitations include the low concentrations of DMEA used in experiments and a restricted range of operational conditions such as temperatures and pressures. Further research is required to extend the study to higher DMEA concentrations and varied conditions to enhance the model's applicability and consider a more advanced activity coefficient model.

Author Contributions: Conceptualization, S.-J.H. and J.-H.W.; methodology, S.-J.H. and J.-H.W.; software, S.-J.H.; validation, S.-J.H.; formal analysis, S.-J.H. and J.Y.H.; investigation, S.-J.H. and J.Y.H.; resources, J.-H.W.; data curation, S.-J.H. and J.Y.H.; writing—original draft preparation, S.-J.H. and J.Y.H.; writing—review and editing, S.-J.H. and J.-H.W.; visualization, S.-J.H.; supervision, J.-H.W.; project administration, J.-H.W.; funding acquisition, S.-J.H. and J.-H.W. All authors have read and agreed to the published version of the manuscript.

Funding: This research was funded by the National Research Foundation of Korea (NRF) grant funded by the Korea government (MSIT) (2021R1C1C2093637 and 2023R1A2C1003698), as well as being supported by the Catholic University of Korea Research Fund, 2024.

Data Availability Statement: Dataset available on request from the authors.

Conflicts of Interest: The authors declare no conflicts of interest.

References

1. Global Carbon Budget. *Global Carbon Budget 2023*; Copernicus Publications: Göttingen, Germany, 2023.
2. Hockstad, L.; Hanel, L. Inventory of US Greenhouse Gas Emissions and Sinks. 2018, Environmental System Science Data Infrastructure for a Virtual Ecosystem. Available online: https://data.ess-dive.lbl.gov/datasets/doi:10.15485/1464240 (accessed on 1 November 2018).
3. 'The Era of Global Boiling Has Arrived,' Says UN Boss, as White House Announces Provisions to Protect Workers from Extreme Heat. Available online: https://cnb.cx/44J1a8k (accessed on 2 September 2024).
4. Patel, S.K.S.; Jeon, M.S.; Gupta, R.K.; Jeon, Y.; Kalia, V.C.; Kim, S.C.; Cho, B.K.; Kim, D.R.; Lee, J.-K. Hierarchical macroporous particles for efficient whole-cell immobilization: Application in bioconversion of greenhouse gases to methanol. *ACS Appl. Mater. Interfaces* **2019**, *11*, 18968–18977. [CrossRef] [PubMed]
5. Fu, S.; Angelidaki, I.; Zhang, Y. In situ biogas upgrading by CO_2-to-CH_4 bioconversion. *Trends Biotechnol.* **2021**, *39*, 336–347. [CrossRef] [PubMed]
6. Song, C.; Liu, Q.; Qi, Y.; Chen, G.; Song, Y.; Kansha, Y.; Kitamura, Y. Absorption-microalgae hybrid CO_2 capture and biotransformation strategy—A review. *Int. J. Greenh. Gas Control.* **2019**, *88*, 109–117. [CrossRef]
7. de Maria, P.D.; Kara, S.; Gallou, F. Biocatalysis in water or in non-conventional media? Adding the CO_2 production for the debate. *Molecules* **2023**, *28*, 6452. [CrossRef] [PubMed]
8. Santamaría, L.; Korili, S.A.; Gil, A. Layered double hydroxides for CO_2 adsorption at moderate temperatures: Synthesis and amelioration strategies. *Chem. Eng. J.* **2023**, *455*, 140551. [CrossRef]
9. Zhu, Z.; Shi, X.; Rao, Y.; Huang, Y. Recent progress of MgO-based materials in CO_2 adsorption and conversion: Modification methods, reaction condition, and CO_2 hydrogenation. *Chin. Chem. Lett.* **2024**, *35*, 108954. [CrossRef]
10. Moon, H.-S.; Moon, J.-H.; Chun, D.H.; Park, Y.C.; Yun, Y.N.; Sohail, M.; Baek, K.; Kim, H. Synthesis of $[Mg_2(DOBDC)(DMF)_2]$@ polystyrene composite and its carbon dioxide adsorption. *Microporous Mesoporous Mater.* **2016**, *232*, 161–166. [CrossRef]
11. Chouikhi, N.; Cecilia, J.A.; Vilarrasa-Garcia, E.; Besghaier, S.; Chlendi, M.; Duro, F.I.F.; Castellon, E.R.; Bagane, M. CO_2 adsorption of materials synthesized from clay minerals: A review. *Minerals* **2019**, *9*, 514. [CrossRef]
12. Miricioiu, M.G.; Zaharioiu, A.; Oancea, S.; Bucura, F.; Raboaca, M.S.; Filote, C.; Ionete, R.E.; Niculescu, V.C.; Constantinescu, M. Sewage sludge derived materials for CO_2 adsorption. *Appl. Sci.* **2021**, *11*, 7139. [CrossRef]

13. Guo, R.-T.; Li, G.-Y.; Liu, Y.; Pan, W.-G. Recent Progress on CO_2 Capture Based on Sterically Hindered Amines: A Review. *Energy Fuels* **2023**, *37*, 15429–15452. [CrossRef]
14. Tatarczuk, A.; Tańczyk, M.; Więcław-Solny, L.; Zdeb, J. Pilot plant results of amine-based carbon capture with heat integrated stripper. *Appl. Energy* **2024**, *367*, 123416. [CrossRef]
15. He, W.; Zhang, S.; Zhu, C.; Fu, T.; Ma, Y. CO_2 chemical absorption into AMP aqueous solution and mass transfer intensification in cascade sudden expansion microchannels. *Chem. Eng. Process.* **2022**, *181*, 109142. [CrossRef]
16. Ji, C.; Yuan, S.; Huffman, M.; El-Halwagi, M.M.; Wang, Q. Post-combustion carbon capture for tank to propeller via process modeling and simulation. *J. CO2 Util.* **2021**, *51*, 101655. [CrossRef]
17. Li, S.; Li, H.; Yu, Y.; Chen, J. Simulation and performance comparison for CO_2 capture by aqueous solvents of n-(2-hydroxyethyl) piperazine and another five single amines. *Processes* **2021**, *9*, 2184. [CrossRef]
18. Raznahan, M.M.; Riahi, S.; Mousavi, S.H. A simple, robust and efficient structural model to predict CO_2 absorption for different amine solutions: Concern to design new amine compounds. *J. Environ. Chem. Eng.* **2020**, *8*, 104572. [CrossRef]
19. Kayahan, E.; Caprio, U.D.; den Bogaert, A.V.; Khan, M.N.; Bulut, M.; Braeken, L.; Gerven, T.V.; Leblebici, M.E. A new look to the old solvent: Mass transfer performance and mechanism of CO_2 absorption into pure monoethanolamine in a spray column. *Chem. Eng. Process. Process Intensif.* **2023**, *184*, 109285. [CrossRef]
20. Kim, J.; Kim, K.; Lim, H.; Kang, J.H.; Park, H.S.; Park, J.; Song, H. Structural investigation of aqueous amine solutions for CO_2 capture: CO_2 loading, cyclic capacity, absorption–desorption rate, and pKa. *J. Environ. Chem. Eng.* **2024**, *12*, 112664. [CrossRef]
21. Li, Q.; Zhang, W.; Qin, Y.; An, A. Model predictive control for the process of mea absorption of CO_2 based on the data identification model. *Processes* **2021**, *9*, 183. [CrossRef]
22. Chen, Y.-H.; Shen, M.-T.; Chang, H.; Ho, C.-D. Control of solvent-based post-combustion carbon capture process with optimal operation conditions. *Processes* **2019**, *7*, 366. [CrossRef]
23. López, A.; La Rubia, M.; Pacheco, R.; Sánchez, S.; Navaza, J.; Gómez-Díaz, D. Carbon dioxide absorption by aqueous mixtures of diisopropanolamine and triethanolamine. *Chem. Eng. Process.* **2016**, *110*, 73–79. [CrossRef]
24. BChoi, K.; Kim, S.-M.; Kim, K.-M.; Lee, U.; Choi, J.H.; Lee, J.-S.; Baek, I.H.; Nam, S.C.; Moon, J.-H. Amine blending optimization for maximizing CO_2 absorption capacity in a diisopropanolamine–methyldiethanolamine–H_2O system using the electrolyte UNIQUAC model. *Chem. Eng. J.* **2021**, *419*, 129517. [CrossRef]
25. Akan, A.P.; Chau, J.; Gullu, G.; Sirkar, K.K. Life Cycle Assessment of Post-Combustion CO_2 Capture and Recovery by Hydrophobic Polypropylene Cross-Flow Hollow Fiber Membrane Contactors with Activated Methyldiethanolamine. *Atmosphere* **2023**, *14*, 490. [CrossRef]
26. Xiao, L.; Qiu, Z.; Feng, S.; Duan, X.; Zhao, Z.; Liu, Y.; Ma, L. Carbon dioxide absorption and desorption experiments based on MDEA. *Chem. Eng. Process.* **2024**, *204*, 109931. [CrossRef]
27. Pinto, D.D.; Zahraee, Z.; Buvik, V.; Hartono, A.; Knuutila, H.K. Vapor liquid equilibrium measurements of two promising tertiary amines for CO_2 capture. *Processes* **2019**, *7*, 951. [CrossRef]
28. Shiva Nagendra, S.M.; Yasa, P.R.; Narayana, M.V.; Khadirnaikar, S.; Rani, P. Mobile monitoring of air pollution using low cost sensors to visualize spatio-temporal variation of pollutants at urban hotspots. *Sustain. Cities Soc.* **2019**, *44*, 520. [CrossRef]
29. Sofia, D.; Giuliano, A.; Gioiella, F.; Barletta, D.; Poletto, M. Modeling of an air quality monitoring network with high space-time resolution. Comput. *Aided Chem. Eng.* **2018**, *43*, 193. [CrossRef]
30. Alam, A.U.; Clyne, D.; Jin, H.; Hu, N.-X.; Deen, M.J. Fully integrated, simple, and low-cost electrochemical sensor array for in situ water quality monitoring. *ACS Sens.* **2020**, *5*, 412. [CrossRef]
31. Lambrou, T.P.; Anastasiou, C.C.; Panayiotou, C.G.; Polycarpou, M.M. A low-cost sensor network for real-time monitoring and contamination detection in drinking water distribution systems. *IEEE Sens. J.* **2014**, *14*, 2765–2772. [CrossRef]
32. Fulton, S.G.; Stegen, J.C.; Kaufman, M.H.; Dowd, J.; Thompson, A. Laboratory evaluation of open source and commercial electrical conductivity sensor precision and accuracy: How do they compare? *PLoS ONE* **2023**, *18*, e0285092. [CrossRef]
33. Thirstrup, C.; Deleebeeck, L. Review on electrolytic conductivity sensors. *IEEE Trans. Instrum. Meas.* **2021**, *70*, 1008222. [CrossRef]
34. Liu, S.; Gao, H.; Luo, X.; Liang, Z. Kinetics and new mechanism study of CO_2 absorption i nto water and tertiary amine solutions by stopped-Flow technique. *AIChE J.* **2019**, *65*, 652–661. [CrossRef]
35. Xiang, J.; Wei, D.; Mao, W.; Liu, T.; Luo, Q.; Huang, Y.; Liang, Z.; Luo, X. Comprehensive kinetic study of carbon dioxide absorption in blended tertiary/secondary amine solutions: Experiments and simulations. *Sep. Purif. Technol.* **2024**, *330*, 125310. [CrossRef]
36. Littel, R.J.; Bos, M.; Knoop, G.J. Dissociation constants of some alkanolamines at 293, 303, 318, and 333 K. *J. Chem. Eng. Data* **1990**, *35*, 276–277. [CrossRef]
37. Kim, S.; Shi, H.; Lee, Y.Y. CO_2 absorption mechanism in amine solvents and enhancement of CO_2 capture capability in blended amine solvent. *Int. J. Greenh. Gas Control.* **2016**, *45*, 181–188. [CrossRef]
38. Shi, H.; Huang, M.; Wu, Q.; Zheng, L.; Cui, L.; Zhang, S.; Tontiwachwuthikul, P. Study of catalytic CO_2 absorption and desorption with tertiary amine DEEA and 1DMA-2p with the aid of solid acid and solid alkaline chemicals. *Molecules* **2019**, *24*, 1009. [CrossRef]
39. Krebs, H.A.; Roughton, F.J.W. Carbonic anhydrase as a tool in studying the mechanism of reactions involving H_2CO_3, CO_2 or HCO_3'. *Biochem. J.* **1948**, *43*, 550. [CrossRef]

40. Kladkaew, N.; Idem, R.; Tontiwachwuthikul, P.; Saiwan, C. Studies on corrosion and corrosion inhibitors for amine based solvents for CO_2 absorption from power plant flue gases containing CO_2, O_2 and SO_2. *Energy Procedia* **2011**, *4*, 1761–1768. [CrossRef]
41. Han, S.J.; Wee, J.H. Comparison of CO_2 absorption performance between methyl-di-ethanolamine and tri-ethanolamine solution systems and its analysis in terms of amine molecules. Greenh. *Gases* **2021**, *11*, 445–460. [CrossRef]
42. Han, S.J.; Wee, J.H. CO_2 absorption performance and electrical properties of 2-amino-2-methyl-1-propanol compared to monoethanolamine solutions as primary amine-based absorbents. *Energy Fuels* **2021**, *35*, 3197–3207. [CrossRef]
43. Han, S.J.; Wee, J.H. Estimation of the Amount of CO_2 Chemically Absorbed in Real Time by Measuring the Electrical Conductivity Variation of Monoethanol-Amine Aqueous Solutions. *Energy Fuels* **2023**, *37*, 19715–19725. [CrossRef]
44. Prini, R.F.; Harvey, A.H.; Palmer, D.A. *Aqueous Systems at Elevated Temperatures and Pressures: Physical Chemistry in Water, Steam and Hydrothermal Solutions*; Elsevier: Amsterdam, The Netherlands, 2004.
45. Rice, E.W.; Bridgewater, L.; American Public Health Association. *Standard Methods for the Examination of Water and Wastewater*; American Public Health Association: Washington, DC, USA, 2012; Volume 10.
46. Debye, P.; Hückel, E. De la theorie des electrolytes. I. abaissement du point de congelation et phenomenes associes. *Phys. Z.* **1923**, *24*, 185–206.
47. Davies, C.; Malpass, V. Ion association and the viscosity of dilute electrolyte solutions. Part 1.—Aqueous inorganic salt solutions. *Trans. Faraday Soc.* **1964**, *60*, 2075–2084. [CrossRef]
48. Stumm, W.; Morgan, J.J. *Aquatic Chemistry: Chemical Equilibria and Rates in Natural Waters*; John Wiley & Sons: Hoboken, NJ, USA, 2013.
49. Felippe, A.C.; Bellettini, I.C.; Eising, R.; Minatti, E.; Giacomelli, F.C. Supramolecular complexes formed by the association of poly (ethyleneimine)(PEI), sodium cholate (NaC) and sodium dodecyl sulfate (SDS). *J. Braz. Chem.* **2011**, *22*, 1539–1548. [CrossRef]
50. Corti, H.R.; Trevani, L.N.; Anderko, A. *Transport Properties in High Temperature and Pressure Ionic Solutions, in Aqueous Systems at Elevated Temperatures and Pressures*; Elsevier: Amsterdam, The Netherlands, 2004; pp. 321–375.
51. Artemov, V.; Volkov, A.; Sysoev, N.; Volkov, A. On autoionization and pH of liquid water. *Dokl. Phys.* **2016**, *61*, 1–4. [CrossRef]
52. de Myttenaere, A.; Golden, B.; Grand, B.L.; Rossi, F. Mean absolute percentage error for regression models. *Neurocomputing* **2016**, *192*, 38–48. [CrossRef]
53. Jiang, W.; Gao, H.; Liang, Z.; Liu, B.; Tontiwachwuthikul, P.; Hu, X. A comparative kinetics study of CO_2 absorption into aqueous DEEA/MEA and DMEA/MEA blended solutions. *AIChE J.* **2018**, *64*, 1350–1358. [CrossRef]
54. Henni, A.; Li, J.; Tontiwachwuthikul, P. Reaction kinetics of CO_2 in aqueous 1-amino-2-propanol, 3-amino-1-propanol, and dimethylmonoethanolamine solutions in the temperature range of 298–313 K using the stopped-flow technique. *Ind. Eng. Chem. Res.* **2008**, *47*, 2213–2220. [CrossRef]
55. Tong, C.; Perez, C.C.; Chen, J.; Marcos, J.-C.V.; Neveux, T.; Moullec, Y.L. Measurement and calculation for CO_2 solubility and kinetic rate in aqueous solutions of two tertiary amines. *Energy Procedia* **2013**, *37*, 2084–2093. [CrossRef]
56. Liu, B.; Luo, X.; Liang, Z.; Olson, W.; Liu, H.; Idem, R.; Tontiwachwuthikul, P. The development of kinetics model for CO_2 absorption into tertiary amines containing carbonic anhydrase. *AIChE J.* **2017**, *63*, 4933–4943. [CrossRef]
57. Kaur, D.P.; Yamada, K.; Park, J.-S.; Sekhon, S.S. Correlation between ion diffusional motion and ionic conductivity for different electrolytes based on ionic liquid. *J. Phys. Chem. B* **2009**, *113*, 5381–5390. [CrossRef]
58. Zhang, A.; Yang, X.; Yang, F.; Zhang, C.; Zhang, Q.; Duan, G.; Jiang, S. Research progress of the ion activity coefficient of polyelectrolytes: A review. *Molecules* **2023**, *28*, 2042. [CrossRef] [PubMed]
59. Jeon, H.-N.; Shin, H.K.; Hwang, S.; No, K.T. Development of an Infinite Dilution Activity Coefficient Prediction Model for Organic Solutes in Ionic Liquids with Modified Partial Equalization Orbital Electronegativity Method Derived Descriptors. *ACS Omega* **2021**, *6*, 15361–15373. [CrossRef] [PubMed]
60. Zhu, L.; Schade, G.W.; Nielsen, C.J. Real-time monitoring of emissions from monoethanolamine-based industrial scale carbon capture facilities. *Environ. Sci. Technol.* **2013**, *47*, 14306–14314. [CrossRef] [PubMed]
61. Chan, C.W.; Zhou, Q.; Tontiwachiwuthikul, P. Part 4a: Applications of knowledge-based system technology for the CO_2 capture process system. *Carbon Manag.* **2012**, *3*, 69–79. [CrossRef]

Disclaimer/Publisher's Note: The statements, opinions and data contained in all publications are solely those of the individual author(s) and contributor(s) and not of MDPI and/or the editor(s). MDPI and/or the editor(s) disclaim responsibility for any injury to people or property resulting from any ideas, methods, instructions or products referred to in the content.